Inhalation Toxicology, 15:1387–1419, 2003

ISSN: 0895-8378 print / 1091-7691 online
DOI: 10.1080/08958370390248888

Taylor & Francis
healthsciences

# COMPARISON OF CALIDRIA CHRYSOTILE ASBESTOS TO PURE TREMOLITE: INHALATION BIOPERSISTENCE AND HISTOPATHOLOGY FOLLOWING SHORT-TERM EXPOSURE

**David M. Bernstein**

Consultant in Toxicology, Geneva, Switzerland

**Jörg Chevalier**

EPS Experimental Pathology Services AG, Muttenz, Switzerland

**Paul Smith**

Research and Consulting Company Ltd., Füllinsdorf, Switzerland

*The differences between chrysotile asbestos, a serpentine mineral, and amphibole asbestos have been debated extensively. Many studies have shown that chrysotile is cleared from the lung more rapidly than amphibole. In order to quantify the comparative clearance of chrysotile and the amphibole asbestos tremolite, both fibers were evaluated in an inhalation biopersistence study that followed the European Commission recommended guidelines. In addition, the histopathological response in the lung was evaluated following the short-term exposure. This article presents the results of this study through 90 days after cessation of exposure. Following the termination of the study, a subsequent article will provide the complete results through 12 mo after cessation of exposure. In order to quantify the dynamics and rate by which these fibers are removed from the lung, the biopersistence of a sample of commercial grade chrysotile from the Coalinga mine in New Idria, CA, of the type Calidria RG144 and of a long-fiber tremolite were studied. For synthetic vitreous fibers, the biopersistence of the fibers longer than 20 μm has been found to be directly related to their potential to cause disease. This study was designed to determine lung clearance (biopersistence) and the histopathological response. As the long fibers have been shown to have the greatest potential for pathogenicity, the aerosol generation technique was designed to maximize the number of long respirable fibers. The chrysotile samples were specifically chosen to have 200 fibers/cm$^3$ longer than 20 μm in length present in the exposure aerosol. These longer fibers were found to be largely composed of multiple shorter fibrils. The tremolite samples were chosen to have 100 fibers/cm$^3$ longer than 20 μm in length present in the exposure aerosol. Calidria chrysotile fibers clear from the lung more rapidly ($T_{1/2,\ fibers\ L>20\ \mu m}$ = 7 h) than any other commercial fiber tested including synthetic vitreous fibers. With such rapidly clearing fibers, the 5-day exposure would not be expected to result in any pathological change in the lung, and the lungs of animals that inhaled Calidria chrysotile showed no sign of inflammation or pathology and were no different than the lungs of those animals that breathed filtered air. Following this 5-day exposure to tremolite, the tremolite fibers once deposited in the lung parenchyma do not clear and almost immediately result in inflammation and a pathological response in the lung. At the first time point examined, 1 day after cessation of exposure, inflammation was*

Received 10 June 2003; accepted 20 July 2003.
This research was sponsored by a grant from the Union Carbide Corporation.
Address correspondence to Dr. David M. Bernstein, Consultant in Toxicology, 40 chemin de la Petite-Boissiere, 1208 Geneva, Switzerland. E-mail: davidb@itox.ch

*observed and granulomas were already formed. By 14 days postexposure these microgranulomas had turned fibrotic, and by 90 days postexposure the severity of the collagen deposits had increased and interstitial fibrosis was observed in one of the rats. These findings provide an important basis for substantiating both kinetically and pathologically the differences between chrysotile and the amphibole tremolite. As Calidria chrysotile has been certified to have no tremolite fiber, the results of the current study together with the results from toxicological and epidemiological studies indicate that this fiber is not associated with lung disease.*

The differences between chrysotile asbestos, a serpentine mineral, and amphibole asbestos have been debated extensively. Many studies have shown that chrysotile is not of the same potency as the amphiboles and is cleared from the lung more rapidly than amphibole (Howard, 1984; Churg & DePaoli, 1988; Mossman et al., 1990; Morgan, 1994; Churg, 1994; McDonald et al., 1999, 2002, 2003; McDonald & McDonald, 1997; McDonald, 1998; Rodelsperger et al., 1999; Hodgson & Darnton, 2000). In order to quantify the comparative clearance of chrysotile and the amphibole asbestos tremolite, both fibers were evaluated in a inhalation biopersistence study which followed the European Commission recommended guidelines (Bernstein & Riego-Sintes, 1999). The biopersistence of synthetic mineral fibers has been shown to be a good predictor of the pathogenic effects following both chronic inhalation and intraperitoneal injection studies in rats (Bernstein et al., 2001a, 2001b). In addition, the histopathological response in the lung was evaluated following the short-term exposure. This article presents the results of this study through 90 days after cessation of exposure. Following the termination of the study, a subsequent article will provide the complete results through 12 mo after cessation of exposure.

The exposure and in-life phases of the study were performed at the Research and Consulting Company Ltd., Füllinsdorf, Switzerland. Fiber counting and sizing were performed under subcontract to RCC at Gesellschaft für Schadstoffmessung und Auftragsanalytik GmbH (GSA), Neuss, Germany.

## METHODS

### Chrysotile and Tremolite Sample Characteristics

The chrysotile studied was obtained from the Coalinga mine in New Idria, CA, of the commercial product Calidria type RG144, which was produced by Union Carbide. This is the same type of chrysotile evaluated by Muhle et al. (1987) and Ilgren and Chatfield (1997, 1998a, 1998b; Ilgren, 2002) and that was found not to produce excess tumors following chronic inhalation in rats. Chrysotile samples from the same mine have been analyzed for purity using chemical separation procedures to concentrate and extract fibers other than chrysotile. The results of this examination of samples from both mining and processing operations revealed that the only asbestos mineral detectable was chrysotile and that no tremolite was present in the asbestos from this mine (Pooley, 2003; Coleman, 1996).

The tremolite sample was obtained from Dr. Alan Jones of the Institute of Occupational Medicine, Edinburgh, Scotland. Davis et al. (1985) evaluated a similar sample in a chronic inhalation study in rats and found that rats treated with tremolite developed very high levels of pulmonary fibrosis as well as 16 carcinomas and 2 mesotheliomas in a group of 39 animals.

The chemical composition and the structure of chrysotile are markedly different from that of amphiboles such as tremolite (Table 1). X-ray diffraction studies of Calidria chrysotile show that it consists of a brucitelike layer with octahedral coordination of its cations coupled to tridymite layer of silicate tetrahedra and curled into a hollow cylinder typical of normal chrysotile fibers (Mumpton & Thompson, 1975; Campbell et al., 1980; Wicks & O'Hanley, 1988). The chemistry of chrysotile is composed of a silicate sheet of composition $(Si_2O_5)_n^{2n-}$, in which three of the O atoms in each tetrahedron are shared with adjacent tetrahedra and a nonsilicate sheet of composition $[Mg_3O_2(OH)_4]_n^{2n+}$. In chrysotile the distances between apical oxygens in a regular (idealized) silicate layer are shorter (0.305 nm) than the O–O distances in the ideal Mg-containing layer (0.342 nm), which may account for the curling of the layers which results in the rolling up like a carpet to form concentric hollow cylinders (Skinner et al., 1988) as illustrated in Figure 1. A transmission electron micrograph showing the rolled structure of chrysotile is shown in Figure 2 (adapted from Skinner et al., 1988) along with a illustration of the rolled nature of the fiber. The Mg molecule is on the outside of the curl and is thus exposed to the surrounding environment of the lung fluid. Hume and Rimstidt (1992) have described the dissolution of chrysotile (Thetford Mine) as occurring in two steps. First the magnesium hydroxide layer which is closest to the fiber surface (Smith, 1974) is removed by rapid

**TABLE 1.** Typical chemical composition (percent)

| Compound | Chrysotile[a] | Tremolite[b] |
|---|---|---|
| $SiO_2$ | 39.77 | 55.10 |
| $Al_2O_3$ | 0.66 | 1.14 |
| $Fe_2O_3$ | 2.02 | 0.32 |
| FeO | ND | 2.00 |
| MnO | 0.07 | 0.10 |
| MgO | 40.62 | 25.65 |
| CaO | 0.32 | 11.45 |
| $K_2O$ | ND | 0.29 |
| $Na_2O$ | 0.01 | 0.14 |
| $H_2O^+$ | 12.69 | 3.52 |
| $H_2$ | 1.54 | 0.16 |
| $CO_2$ | 0.78 | 0.06 |
| Total | 98.4 | 99.93 |

*Note.* ND, not detected.
[a]Campbell et al. (1980).
[b]Hodgson (1979, pp. 80–81).

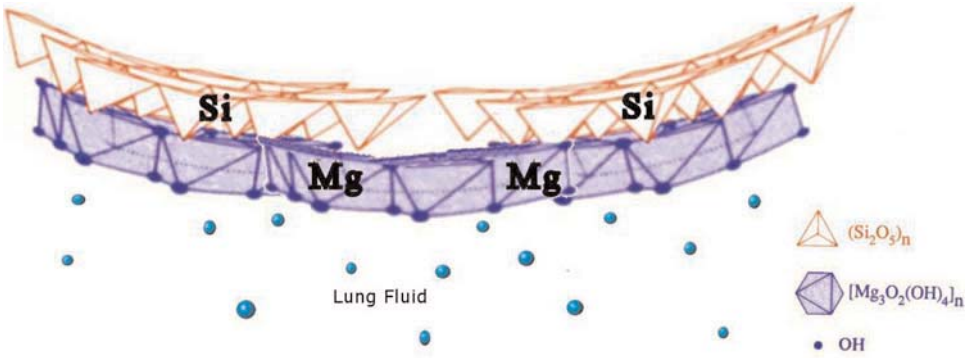


**FIGURE 1.** Schematic representation of the chemical structure of chrysotile showing the Mg molecule is on the outside of the curl facing the lung fluid (light blue droplets). Adapted from Skinner et al. (1988).

leaching; then the silica layer dissolves at a slower rate. The acid pH of the macrophage vacuole may accelerate this process and/or destabilize the chrysotile structure allowing for either separation into the smaller base fragments or breakage of the longer fibers.

The Calidria chrysotile fibrils have been documented as being very short, having a small diameter, thereby reducing its cohesive properties and having a specific surface area that is three to four times as great as other commercial short fiber chrysotile (Mumpton & Thompson, 1975).

In contrast, with amphiboles such as tremolite, the basic structure is in the form of an I-beam with corner-linked $(SiO_4)^{4-}$ tetrahedra linked together in a double-tetrahedral chain that sandwiches a layer with the $Ca_2Mg_5$. In contrast to chrysotile, with tremolite, the Mg is locked within the I-beam structure. This is illustrated in Figure 3.

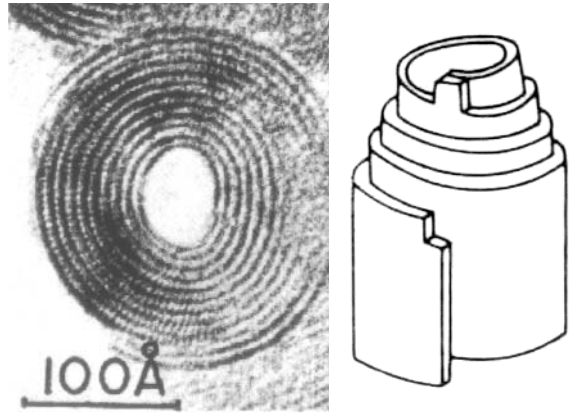


**FIGURE 2.** Transmission electron micrograph of chrysotile showing the curled sheetlike form of the fibers (Skinner et al., 1988) next to an illustration of the tolled structure of chrysotile. Adapted from http://www.a-m.de/englisch/lexikon/mineral/schichtsilicate/chrysotil-kris1.htm.

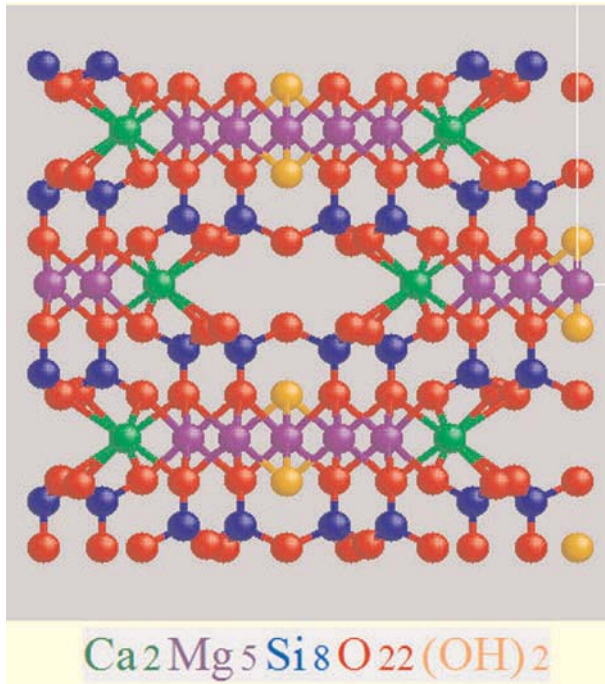


**FIGURE 3.** Schematic representation of the chemical structure of tremolite. The view is down the *c* axis, so that the double chains of silica tetrahedra are oriented into the page. The large hole in the middle is known as the A site, which is vacant in tremolite. http://geo.ucalgary.ca/~tmenard/crystal/trem.html

## Experimental Design

The experimental design of the in-life and biopersistence analysis has been presented in detail previously (Bernstein et al., 1994) and is summarized next. In particular, details of the counting and sizing procedures are reiterated as these are considered essential to the successful interpretation of these studies.

**Animal Exposure** Groups of 56 weanling (~8 wk old) male rats were exposed by flow-past nose-only exposure to a target fiber aerosol concentration for the Calidria chrysotile of 200 fibers L > 20 μm/cm$^3$ and for tremolite of 100 fibers L > 20 μm/cm$^3$ for 6 h/day for a period of 5 consecutive days. A chrysotile concentration twice that required by the EC Biopersistence Protocol was used in order to assure that there was no question of sufficient long fiber exposure. In addition, a negative control group was exposed in a similar fashion to filtered air. To be comparable with current and previous fiber inhalation studies, Wistar rats (HanBrl:WIST, specific pathogen free) were used that were obtained from RCC Ltd, Biotechnology and Animal Breeding Division, Füllinsdorf, Switzerland.

**Exposure System** The fiber aerosol generation system was designed to loft the bulk fibers without breaking, grinding or contaminating the fibers (Bernstein et al., 1994). The animals were exposed by the flow-past nose/

snout-only inhalation exposure system. This system was derived from Cannon et al. (1983) and is different from conventional nose-only exposure systems in that fresh fiber aerosol is supplied to each animal individually and exhaled air is immediately exhausted.

**Fiber Clearance** At 0 days (immediately after the cessation of exposure), 1 day, 2 days, 7 days, 2 wk, 1 mo, 3 mo, 6 mo, and 12 mo postexposure, the lungs from subgroups of animals were weighed and then digested by low-temperature plasma ashing and subsequently analyzed by transmission electron microscopy (at the GSA Corp.) for total chrysotile fibers number in the lungs and chrysotile fiber size (length and diameter) distribution in the lungs. The 6-mo and 12-mo time points are yet to be completed and will be reported subsequently.

**Clinical Examination and Body Weights** All animals were observed for mortality/moribundity twice daily, prior to and following exposure and at least once daily during the acclimatization period and the 12-mo observation period. Clinical signs were recorded during the 5-day exposure period twice daily, prior to and following exposure, and after cessation of exposure once weekly during the first month and every second week thereafter. All animals were sacrificed by exsanguination following deep anesthesia by intraperitoneal injection of sodium pentobarbital (approximately 300 mg/kg). Each animal was weighed on day 1 (used for randomization) and day 8 of the acclimatization period, on days 1, 3, and 5 of the exposure period, once weekly during the month following the last day of exposure and every second week thereafter.

**Histopathology** At 1, 2, 14, and 90 days (and 6 and 12 mo, which are to be completed), separate subgroups of animals were taken for histopathological examination of the respiratory tract. At necropsy, the lungs were weighed and then the left lobe of the lung of each animal was inflated through a bronchial cannula with a neutral buffered 4% formaldehyde solution (formalin). The mediastinal lymph nodes were also fixed in formalin. The lung and lymph nodes were processed, embedded in paraffin, cut at a nominal thickness of 2–4 μm, and stained with hematoxylin and eosin for histopathological examination. In addition, sections of the lung were also stained with Masson's trichrome for collagen evaluation. All abnormalities were described and reported and gross observations were when possible correlated with microscopic findings. The remaining lung lobes were preserved by Rogers Imaging Company (Needham, MA) for optional examination by confocal microscopy.

In the scoring system used for individual pathologic diagnoses, the histological changes were described according to distribution, severity, and morphologic character. The severity was scored as minimal, slight, moderate, marked, or massive (grades 1–5, respectively).

### Lung Digestion for Fiber/Particle Analysis

From 5 rats per group per time point the lungs were frozen at necropsy at minus 20°C. The frozen lungs were subsequently dehydrated by freeze-dry-

ing (Edwards EF4 Modulyo freeze dryer) and dried to constant weight to determine the dry weight of the tissue. The dry tissue was plasma ashed in a Plasma systems 200 (Technics Plasma GmbH) for at least 16 h. Upon removal from the ashing unit, the ash from each lung was weighed and suspended in 10 ml methanol using a low intensity ultrasonic bath. The suspension was then transferred into a glass bottle with the combustion boat rinse and the volume made up to 20 ml. An aliquot was then removed and filtered onto a gold-coated polycarbonate filter (pore size of 0.2 μm).

### Counting Rules for the Evaluation of Air and Lung Samples by Transmission Electron Microscopy

All fibers visible at a magnification of 10,000× were taken in consideration. All objects seen at this magnification were sized with no lower or upper limit imposed on either length or diameter. The bivariate length and diameter was recorded individually for each object measured. Fibers were defined as any object that had an aspect ratio of at least 3:1. The diameter was determined at the greatest width of the object. All other objects were considered as nonfibrous particles.

The stopping rules for counting of each sample were defined as follows: For nonfibrous particles, the recording of particles was stopped when a total of 30 particles were recorded. For fibers, the recording was stopped when 500 fibers with length $\geqslant$5 μm, diameter $\leqslant$3 μm (often referred to as WHO fibers; WHO, 1985) or a total of 1000 fibers and nonfibrous particles were recorded. If this number of fibers was not reached after evaluation of 0.15 $mm^2$ of filter surface, additional fields of view were counted until either 500 WHO fibers were reached or a total of 5 $mm^2$ of filter surface was evaluated, even if a total of 500 countable WHO fibers was not reached. The evaluation of objects of length <5 μm was stopped when 100 objects were reached.

### Validation of the Lung Digestion and Counting Procedures

Something that is essential to the validity of this type of study and that is absent from nearly all other studies of chrysotile is the validation of the lung digestion and counting procedures in terms of fiber recovery and not significantly altering the fiber length distribution.

The only method suitable for validation of chrysotile fiber recovery would be a parallel analysis using a noninvasive measurement technique such as confocal microscopy (Bernstein et al., 2003). To validate the procedures, the lungs from three rats exposed at the same time and under the same conditions as mentioned and sacrificed at 1 day after cessation of exposure were analyzed.

At necropsy the lungs were removed and were fixed in Karnovski's fixative by gentle instillation under a pressure of 30 cm $H_2O$ with simultaneous immersion in fixative. The trachea was then ligated and the inflated lungs were stored in the same fixative. Following fixation, apical lobes were divided into 5 pieces (10 $mm^2$ × 5 mm thick) cut parallel to the hilum, dehydrated in

graded ethanolic series to absolute, stained with 0.005% lucifer yellow, and embedded in Spurr plastic for microscopic analysis (Rogers et al., 1999). Flat surfaces were prepared from hardened plastic blocks containing embedded lung pieces.

Confocal microscopy was performed on three randomly selected animals from each time point using Sarastro 2000 (Molecular Dynamics, Inc.) laser scanning microscopes fitted with 25-mW argon-ion lasers and an upright microscope (Optiphot-2; Nikon, Inc., or Zeiss Axiophot) modified for reflected light imaging. These confocal microscopes were used to record image data in dual channel reflected and fluorescent imaging mode. Optical bench settings for the Sarastro 2000 CLSMs were: excitation 488 nm (lucifer yellow), emission 488 nm notch (±2 nm) and a 510-long pass filter, laser power 12–15 mW, 30% transmission, photomultiplier voltage set between 500 and 800 V. Fluorescently labeled cellular constituents and reflective/refractive fibers (and particles) were imaged simultaneously with this arrangement. Each "exposure" produced two digital images in perfect register with one another.

An image recorded in either mode was a two-dimensional ($x,y$), 512 × 512 array of pixels, each with an intensity value from 0 to 254 gray scale units (a value of 255 indicated saturation of the intensity scale). Optical ($x,y$) sections, individually and in depth series, were recorded at various positions along the $z$ axis by adjusting the stage height using stepper motors under computer control. Images and image series were analyzed and prepared for presentation by employing specialized computer software. Images were recorded through 40× objectives. The dimensions of pixels in the recorded volume were ($x$, $y$, and $z$ dimensions, respectively) 0.13 μm, 0.13 μm, and 0.3 μm.

Our procedure was to place the microscope objective at random over the lung specimen exposed at the surface of the epoxy embedment, collect a depth series of images, return to the initial starting depth, move two field widths in the positive $x$ direction, and repeat the process. Twenty-five depth series per piece of lung (for a total of 100 fields of view per animal) were obtained in this way. (If the perimeter of the lung section was encountered, the objective was moved two field widths in the positive $y$ direction, and the stepping was continued in the negative $x$ direction.)

The number and length of fibers in each volume was counted by a human operator who was able to move up and down through the depth series of images while looking for the characteristic bright points or lines that indicated a reflective or refractile particle or fiber.

## RESULTS

### Validation of Lung Digestion Procedure

To assure that the lung digestion and transmission electron microscopy (TEM) procedures used in this study did not affect the fiber length of the chrysotile present in the lung, 3 additional rats sacrificed on day 1 were examined for fiber length distribution by confocal microscopy. As mentioned earlier, confocal microscopy allows detection of the fibers present in the lung

in a three-dimensional cube of the lung tissue and is noninvasive. Thus, if the longer fibers were affected by the lung digestion procedure, this would be evident from the confocal measurements.

As the confocal microscope has a limit of detection of approximately 0.13 μm, the TEM data were examined and showed that all fibers less than 0.13 μm in diameter were shorter than 10 μm in length. Thus, all longer fibers could be detected by the confocal procedure.

The results of this analysis confirmed that there is a very good correlation between the length distribution as measured by the lung digestion procedure/TEM and the confocal methodology with a correlation $r^2 = .9$ and that the TEM procedure does not reduce the length distribution of the fibers seen in the confocal analysis.

### Inhalation Biopersistence

The EC Inhalation Biopersistence Protocol specifies that the exposure atmosphere to which the animals are exposed should have at least 100 fibers/$cm^3$ longer than 20 μm. In this study, the number of fibers longer than 20 μm in the chrysotile exposure atmosphere was purposely increased to a mean of 200 fibers with L > 20 μm/$cm^3$, in order to maximize any potential effect of these long fibers on clearance from the lung. For tremolite the mean exposure concentration was maintained at 100 fibers with L > 20 μm/$cm^3$. The number, concentration, and size distribution of the air control, chrysotile, and tremolite exposure groups are shown in Table 2.

The mean number of WHO fibers in the chrysotile exposure atmosphere was 11,053 fibers/$cm^3$, which was more than 100,000 times the OSHA occupational exposure limit for chrysotile of 0.1 fibers/$cm^3$. The tremolite exposure atmosphere had fewer shorter fibers resulting in a mean of 1090 WHO fibers/$cm^3$. The mean total number of fibers of all sizes present in the exposure atmosphere was 48,343 fibers/$cm^3$ for chrysotile and 3128 fibers/$cm^3$ for tremolite.

The bivariate length and diameter distribution of each fiber measured according to the counting rules already described was recorded. The aerosol generation technique was designed to maximize the number of long respirable fibers. As illustrated in Figures 4 and 6 for chrysotile and tremolite respectively, 99% of the chrysotile fibers in the exposure atmosphere were less than 0.4 μm in diameter while 98% of the tremolite fibers were less than 1.0 μm and thus potentially respirable in the rat. Of the longer fibers (L > 20 μm), 99% of the long chrysotile fibers were also less than 0.4 μm in diameter while 75% of the long tremolite fibers were less than 1.0 μm in diameter.

Figures 5 and 7 show for chrysotile and tremolite respectively the bivariate length and diameter distribution of the fibers recovered from the lung at 1 day following cessation of exposure. The mean fiber concentrations and dimensions are presented in Tables 4 and 5 for each time point.

It is interesting to note that for the chrysotile fibers the diameter distribution in the lung at 1 day after cessation of exposure (GMD 0.11, range 0.03–2.5 μm) has a greater spread in comparison to that found in the aerosol

**TABLE 2.** The number, concentration, and size distribution of the chrysotile, tremolite, and air control exposure atmosphere

| Exposure group | Gravimetric concentration ($mg/m^3$), mean ± standard deviation | Mean number of fibers evaluated | Mean number of total fibers/ $cm^3$ | Mean number WHO fibers/ $cm^3$ | Mean percent WHO fibers of total fibers | Mean number of fibers L > 20 $\mu m/^3 cm^3$ |
|---|---|---|---|---|---|---|
| Calidria chrysotile | 1.69 ± 0.28 | 2016 | 48,343.2 | 11,052.8 | 22.2 | 190.5 |
| Tremolite | 11.47 ± 1.30 | 1627 | 3128.1 | 1090.3 | 34.9 | 106.2 |
| Air control | 0.00 | 2 | 0.1 | 0 | 0 | 0 |

*Note.* —, Not determined.

(GMD 0.07, range 0.02–0.7 μm). This is a transient effect for which the reason is unknown.

The differences between the chrysotile and tremolite fibers are also seen in the transmission electron micrographs (TEM) of samples collected from the exposure atmosphere to the animals. Figure 8 shows Calidria chrysotile fibers collected from the exposure aerosol.

Figure 9 is a similar TEM of the Calidria fibers of an air sample collected at the King City Mill where Calidria chrysotile was mined. The holes (circles) in both images are inherent to the Nuclepore type filters on which these samples were analyzed and have a uniform diameter of 0.2 μm. In

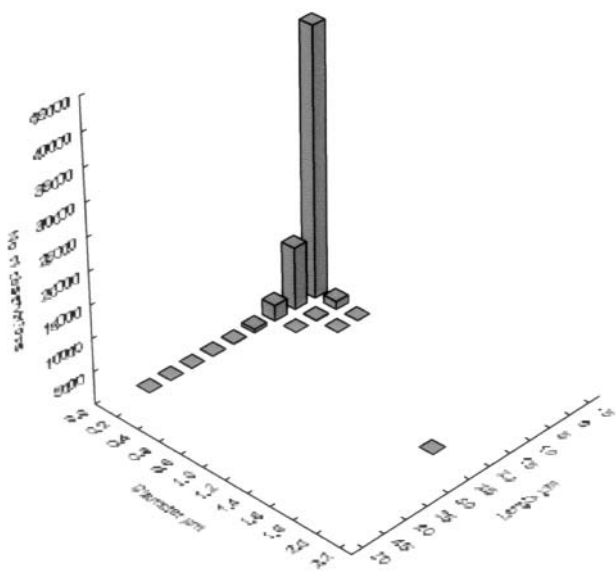

**FIGURE 4.** Bivariate length and diameter histogram of the Calidria chrysotile WHO fibers in the exposure atmosphere (measured by TEM).

| Mean percent fibers L > 20 μm of total fibers | Diameter range (μm) | Length range (μm) | GMD (μm) ± standard deviation | GML (μm) ± standard deviation | Mean diameter (μm) ± standard deviation | Mean length (μm) ± standard deviation |
|---|---|---|---|---|---|---|
| 0.4 | 0.02–0.7 | 0.07–37.6 | 0.07 ± 1.94 | 2.65 ± 3.10 | 0.08 ± 0.07 | 3.61 ± 7.37 |
| 3.4 | 0.1–3.7 | 0.9–75 | 0.27 ± 2.06 | 3.71 ± 3.52 | 0.32 ± 0.45 | 5.49 ± 13.97 |
| 0 | — | — | — | — | — | — |

both images, the longer fibers can be seen to be composed of multiple fibrils of shorter length.

Figure 10 shows a TEM image of the tremolite aerosol fibers, which are uniform cylindrical objects, often with jagged edges where they have been broken from longer fiber strands.

### Fiber Clearance

The Calidria chrysotile fibers longer than 20 μm that deposit in the lung rapidly "disappear" from the lung as shown in Figure 11 with a clearance

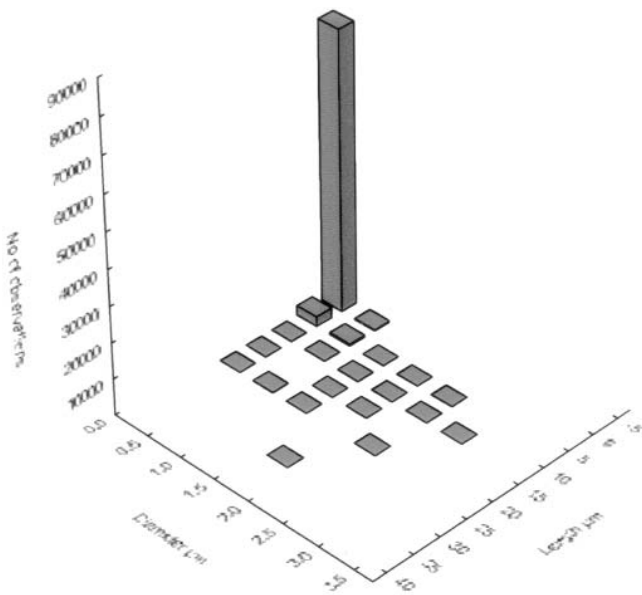


**FIGURE 5.** Bivariate length and diameter histogram of the Calidria chrysotile WHO fibers recovered from the lung within 2 h (day 0) following cessation of exposure (measured by TEM).

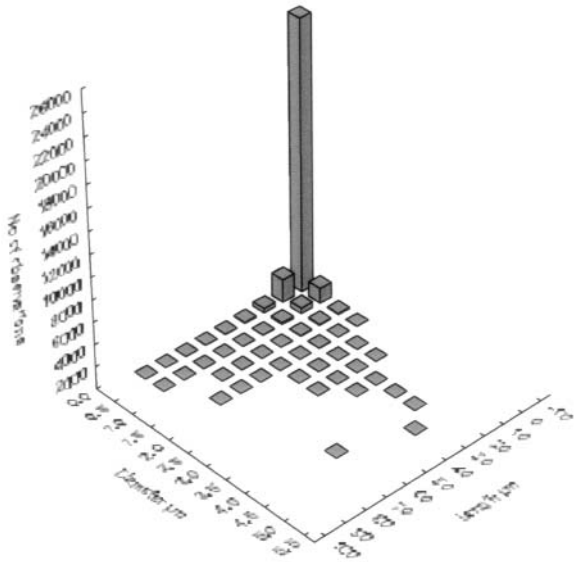

**FIGURE 6.** Bivariate length and diameter histogram of the tremolite WHO fibers in the exposure atmosphere (measured by TEM).

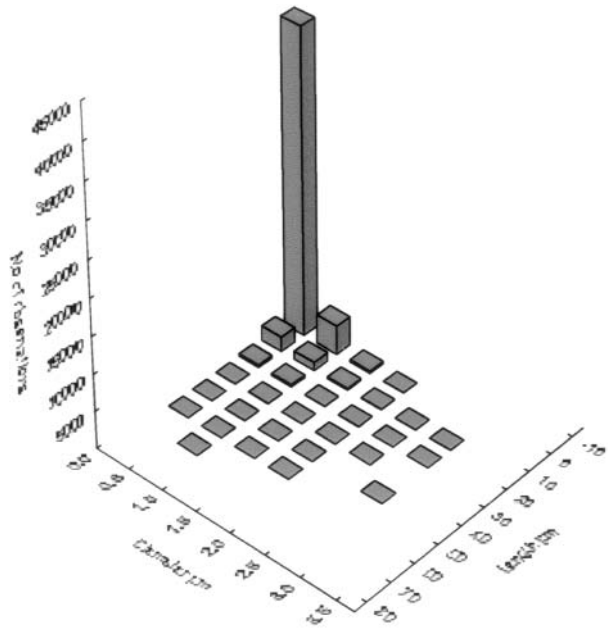

**FIGURE 7.** Bivariate length and diameter histogram of the tremolite WHO fibers recovered from the lung within 2 h (day 0) following cessation of exposure (measured by TEM).

**TABLE 3.** Effects of exposure to Calidria chrysotile

| Days after cessation of exposure | 0 | 1 | 2 | 7 | 14 | 30 | 90 |
|---|---|---|---|---|---|---|---|
| Total number of fibers evaluated | 1517 | 1507 | 1507 | 1415 | 926 | 657 | 527 |
| Mean (± std. dev.) number of total fibers per lung lobe ($\times 10^6$) | 46.06 ± 8.21 | 42.92 ± 5.82 | 37.68 ± 1.53 | 35.34 ± 2.24 | 39.60 ± 2.00 | 32.06 ± 2.74 | 12.76 ± 1.11 |
| Mean (± std. dev.) number of WHO fibers per lung lobe ($\times 10^6$) | 2.26 ± 0.55 | 1.74 ± 0.13 | 1.55 ± 0.10 | 1.05 ± 0.15 | 0.48 ± 0.01 | 0.18 ± 0.06 | 0.03 ± 0.01 |
| Mean WHO fibers of total fibers (%) | 4.9 | 4.1 | 4.1 | 3.0 | 1.2 | 0.5 | 0.2 |
| Mean (± std. dev.) number of fibers L > 20 μm per lung lobe ($\times 10^6$) | 0.01 ± 0.005 | 0.00 | 0.00 | 0.00 | 0.00 | 0.00 | 0.00 |
| Mean fibers L > 20 μm of total fibers (%) | 0.0 | 0.0 | 0.0 | 0.0 | 0.0 | 0.0 | 0.0 |
| Mean (± std. dev.) number of fibers L 5–20 μm per lung lobe ($\times 10^6$) | 2.25 ± 0.55 | 1.74 ± 0.13 | 1.55 ± 0.10 | 1.05 ± 0.15 | 0.48 ± 0.01 | 0.18 ± 0.06 | 0.03 ± 0.01 |
| Mean fibers L 5–20 μm of total fibers (%) | 4.9 | 4.1 | 4.1 | 3.0 | 1.2 | 0.5 | 0.2 |
| Diameter range (μm) | 0.03–2.5 | 0.03–1.9 | 0.03–1.75 | 0.03–1.8 | 0.03–1.4 | 0.03–0.8 | 0.03–0.53 |
| Length range (μm) | 0.56–25 | 0.6–17 | 0.54–14 | 0.52–14 | 0.52–14 | 0.58–11 | 0.5–7.84 |
| Mean diameter (μm) | 0.15 | 0.16 | 0.13 | 0.13 | 0.09 | 0.09 | 0.06 |
| Standard deviation | 0.40 | 0.35 | 0.28 | 0.23 | 0.19 | 0.10 | 0.06 |
| Mean length (μm) | 2.12 | 2.16 | 2.03 | 2.08 | 1.80 | 1.63 | 1.24 |
| Standard deviation | 4.60 | 4.27 | 4.01 | 3.74 | 3.51 | 2.58 | 1.36 |
| GMD (μm) | 0.11 | 0.12 | 0.10 | 0.10 | 0.08 | 0.08 | 0.06 |
| Standard deviation | 3.31 | 3.12 | 2.99 | 2.64 | 2.48 | 2.07 | 1.62 |
| GML (μm) | 1.76 | 1.81 | 1.68 | 1.78 | 1.56 | 1.44 | 1.10 |
| Standard deviation | 3.23 | 3.14 | 3.21 | 2.96 | 2.85 | 2.33 | 1.83 |
| Mean aspect ratio mean | 19.61 | 19.22 | 20.55 | 21.90 | 23.91 | 23.86 | 22.28 |
| Number of particles evaluated | 0.40 | 0.60 | 0.00 | 0.00 | 0.20 | 0.20 | 0.00 |
| Mean number of particles/lung lobe ($\times 10^6$) | 0.00 | 0.01 | 0.00 | 0.00 | 0.00 | 0.00 | 0.00 |
| ≤1 μm particles/lung lobe ($\times 10^6$) | 0.00 | 0.00 | 0.00 | 0.00 | 0.00 | 0.00 | 0.00 |
| >1 μm–≤ 3 μm particles/lung lobe ($\times 10^6$) | 0.00 | 0.00 | 0.00 | 0.00 | 0.00 | 0.00 | 0.00 |
| >3 μm particles/lung lobe ($\times 10^6$) | 0.00 | 0.00 | 0.00 | 0.00 | 0.00 | 0.00 | 0.00 |

**TABLE 4.** Effects of exposure to tremolite

| Days after cessation of exposure | 0 | 1 | 2 | 7 | 14 | 30 | 90 |
|---|---|---|---|---|---|---|---|
| Total number of fibers evaluated | 2022 | 1876 | 1923 | 1848 | 1868 | 687 | 1791 |
| Mean (± std. dev.) number of total fibers per lung lobe ($\times 10^6$) | 68.46 ± 4.72 | 63.89 ± 7.05 | 68.06 ± 4.70 | 63.01 ± 1.98 | 59.55 ± 3.41 | 40.78 ± 4.35 | 32.71 ± 1.72 |
| Mean (± std. dev.) number of WHO fibers per lung lobe ($\times 10^6$) | 17.71 ± 3.36 | 12.83 ± 3.67 | 16.56 ± 3.49 | 13.45 ± 1.24 | 13.77 ± 1.38 | 9.56 ± 2.76 | 7.62 ± 0.53 |
| Mean WHO fibers of total fibers (%) | 25.7 | 19.8 | 24.2 | 21.3 | 23.2 | 24.9 | 23.4 |
| Mean (± std. dev.) number of fibers L > 20 µm per lung lobe ($\times 10^6$) | 1.42 ± 0.26 | 0.82 ± 0.30 | 1.04 ± 3.37 | 0.74 ± 0.12 | 0.77 ± 0.04 | 0.57 ± 0.20 | 0.63 ± 0.08 |
| Mean fibers L > 20 µm of total fibers (%) | 2.1 | 1.3 | 1.5 | 1.2 | 1.3 | 1.4 | 1.9 |
| Mean (± std. dev.) number of fibers L 5–20 µm per lung lobe ($\times 10^6$) | 16.29 ± 3.15 | 12.01 ± 3.41 | 15.53 ± 3.15 | 12.71 ± 1.27 | 13.00 ± 1.37 | 8.99 ± 1.89 | 7.00 ± 0.48 |
| Mean fibers L 5–20 µm of total fibers (%) | 23.7 | 18.6 | 22.7 | 20.1 | 21.9 | 21.7 | 21.5 |
| Diameter range (µm) | 0.056–2.5 | 0.05–2.2 | 0.06–2.2 | 0.044–1.8 | 0.049–2.1 | 0.046–2.0 | 0.032–2.5 |
| Length range (µm) | 0.7–58 | 0.65–60 | 0.7–58 | 0.62–52 | 0.54–54 | 0.51–50 | 0.54–54 |
| Mean diameter (µm) | 0.32 | 0.28 | 0.32 | 0.28 | 0.27 | 0.25 | 0.23 |
| Standard Deviation | 0.38 | 0.38 | 0.35 | 0.32 | 0.35 | 0.33 | 0.34 |
| Mean length (µm) | 4.46 | 3.99 | 4.31 | 3.83 | 4.06 | 4.12 | 4.47 |
| Standard deviation | 12.40 | 11.78 | 12.08 | 10.44 | 10.86 | 10.27 | 10.78 |
| GMD (µm) | 0.26 | 0.23 | 0.27 | 0.23 | 0.23 | 0.21 | 0.18 |
| Standard deviation | 2.14 | 2.27 | 2.09 | 2.13 | 2.17 | 2.18 | 2.36 |
| GML (µm) | 3.10 | 2.82 | 3.04 | 2.71 | 2.79 | 2.73 | 2.88 |
| Standard deviation | 3.86 | 3.85 | 3.77 | 3.75 | 3.79 | 3.66 | 3.82 |
| Mean aspect ratio mean | 15.11 | 15.04 | 14.77 | 15.21 | 15.65 | 17.05 | 19.99 |
| Number of particles evaluated | 4.00 | 4.40 | 4.50 | 5.20 | 4.40 | 4.20 | 4.20 |
| Mean number of particles/lung lobe ($\times 10^6$) | 0.06 | 0.05 | 0.06 | 0.06 | 0.05 | 0.05 | 0.05 |
| ≤1 µm particles/lung lobe ($\times 10^6$) | 0.03 | 0.03 | 0.02 | 0.02 | 0.02 | 0.02 | 0.02 |
| >1 µm–≤3 µm particles/lung lobe ($\times 10^6$) | 0.02 | 0.02 | 0.03 | 0.02 | 0.02 | 0.03 | 0.02 |
| >3 µm particles/lung lobe ($\times 10^6$) | 0.01 | 0.00 | 0.00 | 0.01 | 0.01 | 0.01 | 0.00 |

**TABLE 5.** Lung weights: mean ± standard deviation ($n$ = 7)

| Time postexposure (days) | Group 1 air control | Group 2 Calidria chrysotile | Group 3 tremolite | Statistically significant mean differences[a] |
|---|---|---|---|---|
| 1 | 1.109 ± 0.102 | 1.134 ± 0.104 | 1.297 ± 0.120 | Air-Trem $p$ = .006<br>Calidria-Trem $p$ = .005 |
| 2 | N.W. | 0.971 ± 0.078 | 1.202 ± 0.139 | Calidria-Trem $p$ = .002 |
| 7 | N.W. | 1.066 ± 0.056 | 1.237 ± 0.056 | Calidria-Trem $p$ = .001 |
| 14 | N.W. | 1.138 ± 0.085 | 1.250 ± 0.086 | Calidria-Trem $p$ = .013 |
| 30 | 1.144 ± 0.103 | 1.179 ± 0.049 | 1.340 ± 0.150 | Air-Trem $p$ = .014<br>Calidria-Trem $p$ = 0.019 |
| 90 | N.W. | 1.233 ± 0.159 | 1.381 ± 0.077 | Calidria-Trem $p$ = .047 |

*Note.* N.W., the control group was not weighed at these time points.
[a]Dunnett test based on pooled variance.

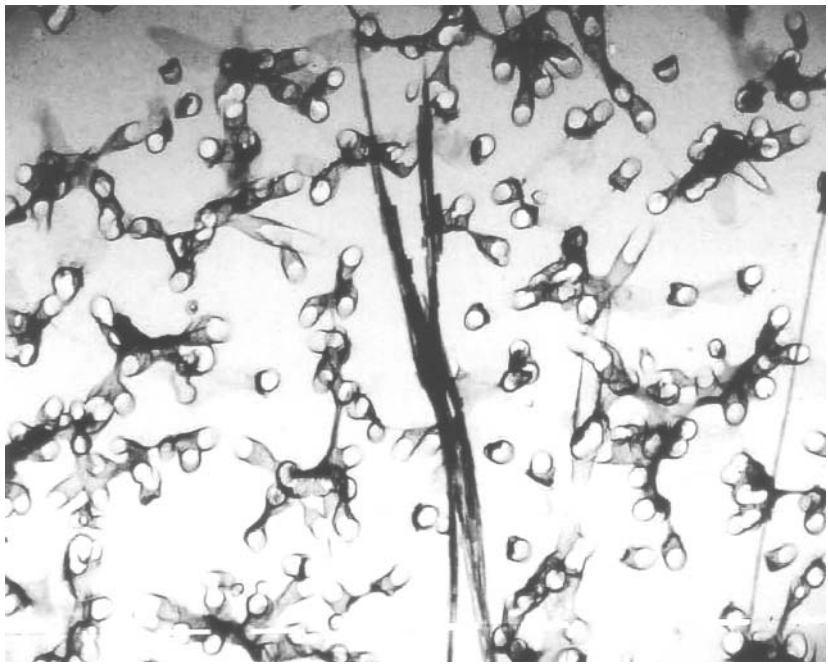

**FIGURE 8.** Transmission electron micrograph of the Calidria chrysotile aerosol sample taken from the exposure atmosphere, magnification 12,500×, showing that the longer Calidria chrysotile fibers can be seen to be composed of multiple fibrils of shorter length. White bar at the bottom of the photo is 0.5 μm in length; the holes in the filter are from the Nucleopore filter material and are approximately 0.2 μm in diameter.

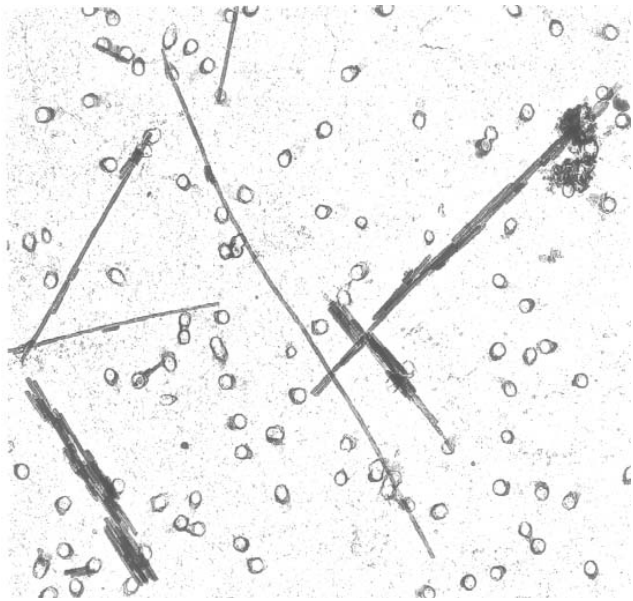

**FIGURE 9.** Transmission electron micrograph of the Calidria chrysotile aerosol sample taken from the King City Mill Air Sample showing that the longer Calidria chrysotile fibers can be seen to be composed of multiple fibrils of shorter length. The holes in the filter are from the Nucleopore filter material and are approximately 0.2 μm in diameter. The King City Mill processed the Calidria chrysotile.

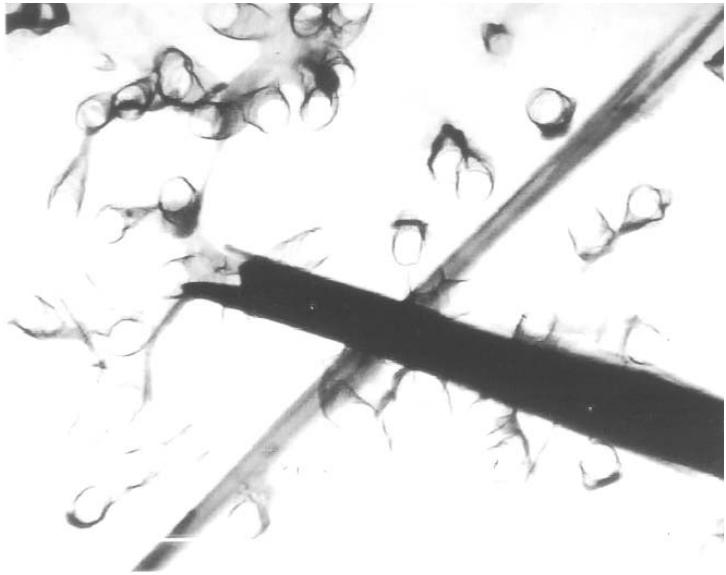

**FIGURE 10.** Transmission electron micrograph of the tremolite aerosol sample taken from the exposure atmosphere, magnification 25,500×, showing the solid density and jagged edges of the tremolite fibers. White bar at the bottom of the photo is 0.5 μm in length; the holes in the filter are from the Nucleopore filter material and are approximately 0.2 μm in diameter.

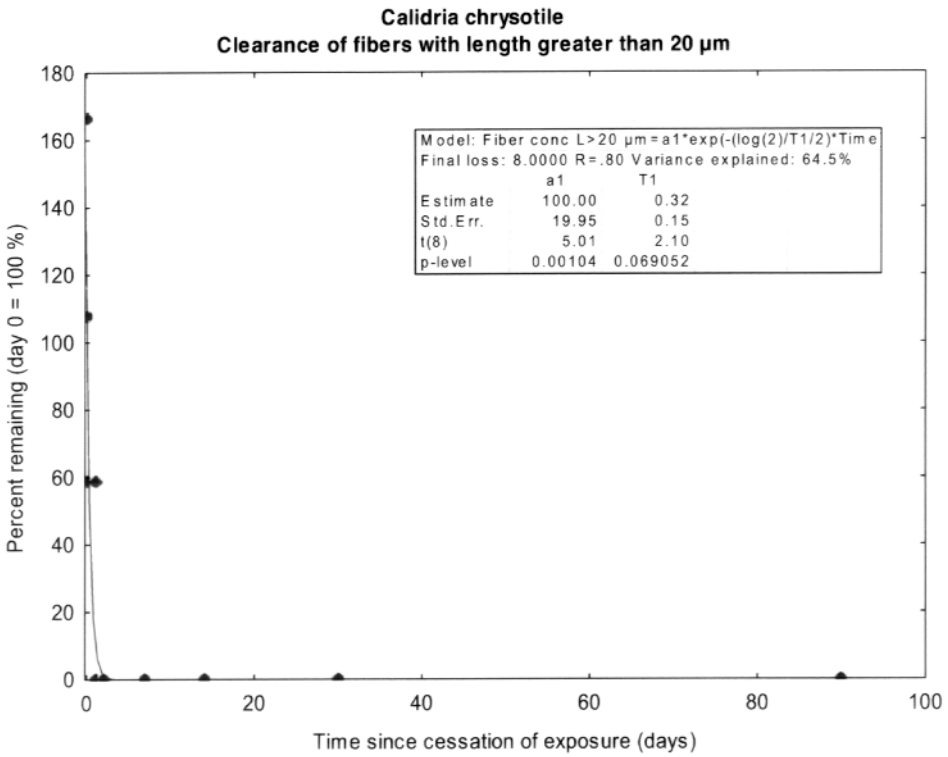


**FIGURE 11.** Graph showing the clearance of the Calidria chrysotile fibers longer than 20 µm from the lung following cessation of the 5-day exposure period. The diamonds indicate the percent remaining of the individual lungs (the mean of day 0 = 100% as nearly all fibers were gone by day 1). The solid line is the clearance curve fitted to the data using nonlinear regression techniques with a single exponential (StatSoft, Inc., 2003). The regression coefficients are presented in insert in the figure.

half-time of the fibers longer than 20 µm of 0.3 days. At the day 0 time point, between 1 and 3 fibers L > 20 µm were counted on the filter. At day 1, 1 fiber L > 20 µm was found in 1 rat and none in the other rats. From day 2 onward, no fibers L > 20 µm were observed. In comparison, 100 fibers L > 20 µm were counted in the tremolite-exposed animals even though they were exposed to one-half the aerosol concentrations of long fibers.

In marked contrast, the longer tremolite fibers (L > 20 µm) that deposit in the lung show an initial shorter term clearance probably associated with the clearance of fibers which deposited in the tracheal-bronchial tree followed by no further clearance. From Figure 12, this shorter term clearance appears to be finished by 7 days after cessation of exposure. Following this early phase, no further clearance occurs of the long tremolite fibers.

The shorter chrysotile fibers with lengths between 5 and 20 µm also clear quickly with a half-time of 7 days (single exponential fit to the data). The objects less than 5 µm in length clear with a half-time of 59 days (single exponential fit to the data); however, as the whole lung was digested for these

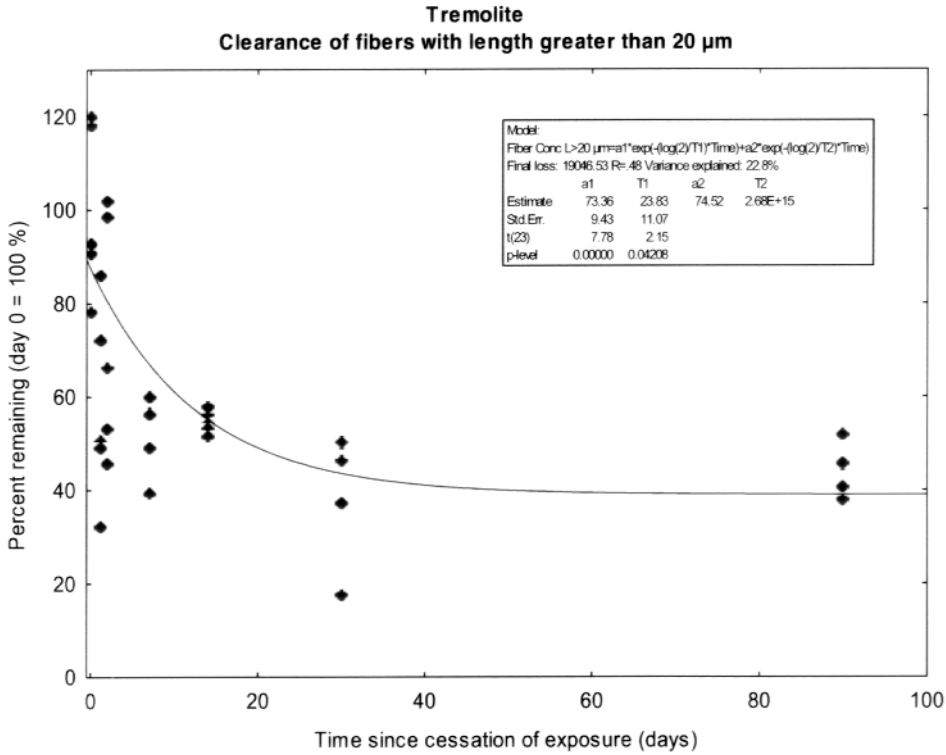


**FIGURE 12.** Graph showing the clearance of the tremolite fibers longer than 20 µm from the lung following cessation of the 5-day exposure period. The diamonds indicate the percent remaining of the individual lungs (the mean of day 1 = 100%). The solid line is the clearance curve fitted to the data using nonlinear regression techniques with a single exponential (StatSoft, Inc., 2003). The regression coefficients are presented in insert in the figure.

measurements, it was not possible to determine in which compartments these shorter objects remained. This clearance rate is within the range reported for the clearance of insoluble nuisance dusts (Muhle et al., 1990; Stöber et al., 1990; Yu et al., 1994; Oberdoerster, 1994).

Again, this is in sharp contrast with the short fiber clearance in the tremolite-exposed rats for which all length fractions show no clearance after the early time points. For the fiber length fraction of 5–20 µm an early clearance phase occurs with a half-time of 27 days leveling off at 40% followed by no further clearance. Similar kinetics are seen for the objects less than 5 µm in length, where the short-term clearance half-time is 21 days, again leveling off thereafter with more than 50% remaining at 90 days.

### Lung Weights

As shown in Table 5, the lung weights measured at necropsy show that following the 5-day exposure, no statistically significant differences were seen between the air control and Calidria chrysotile exposure groups at any time

point. In contrast, even at day 1 postexposure and continuing at each time point through 90 days, there is a statistically significant systematic increase in mean lung weights of the tremolite-exposed animals in comparison to both the air control and chrysotile-exposed animals.

### Histopathological Results

While the fiber clearance results sharply differentiate Calidria chrysotile fiber retention from that of tremolite, the histopathology findings provide a pathological basis for evaluating the importance of this difference.

The summary incidence of the histopathological findings in the lung at days 1, 2, 14, and 90 after cessation of exposure are presented in the Appendix in Tables A1 through A4. Shown are the specific histological findings seen in the lung, the number of animals per dose group examined and the number of animals with each grade of the finding. For each finding the total number of animals affected and the mean severity are also shown.

Microscopically, no findings related to the exposure to Calidria chrysotile were observed at any sacrifice time point. At days 2 and 14 a few rats were noted with foam-cell aggregation. These foam cells are histiocytes in the alveolar lumen. They have a foamy, microvesicular cytoplasm and are arranged in small aggregates close to bronchiolar branches or subpleurally. Such aggregates are commonly observed in control rats (RCC historical control data) and were not considered as exposure related.

In contrast, in the rats exposed to tremolite, a number of cellular lesions were observed mainly at the bronchiolar-alveolar junction at all sacrifice time points. These cellular lesions were characterized by alveolar macrophage aggregation and microgranulomas. In the rats sacrificed after the 1- and 2-day observation periods, alveolar lining cell hypertrophy/hyperplasia and bronchiolitis were noted. At both 14 days and 90 days after cessation of exposure, collagen deposition (fibrosis) was diagnosed in microgranulomas in addition to the cellular lesions. At 90 days after cessation of exposure, the collagen in the granulomas has increased in severity up to grade 3 and interstitial collagen deposition is seen already in 1 animal. These findings are summarized in Table 6.

These lesions are shown in the photomicrographs of the tremolite exposed lungs in Figures 13 through 16. Figure 13 shows the granulomatous response that is already developed at 1 day following cessation of the 5-day exposure

**TABLE 6.** Mean degree of cellular lesions and fibrosis at the different sacrifice time points in rats exposed to tremolite

| Time (days) after cessation of exposure | Figure | Alveolar macrophage | Granulomas | Fibrosis granuloma | Interstitial fibrosis |
|---|---|---|---|---|---|
| 1 day | 10 | 2.4 | 2.6 | 0 | 0 |
| 2 days | | 3.0 | 3.0 | 0 | 0 |
| 14 days | 11 | 2.6 | 3.0 | 1.3 | 0 |
| 90 days | 12 | 2.0 | 2.8 | 2.8 | 0.5 |

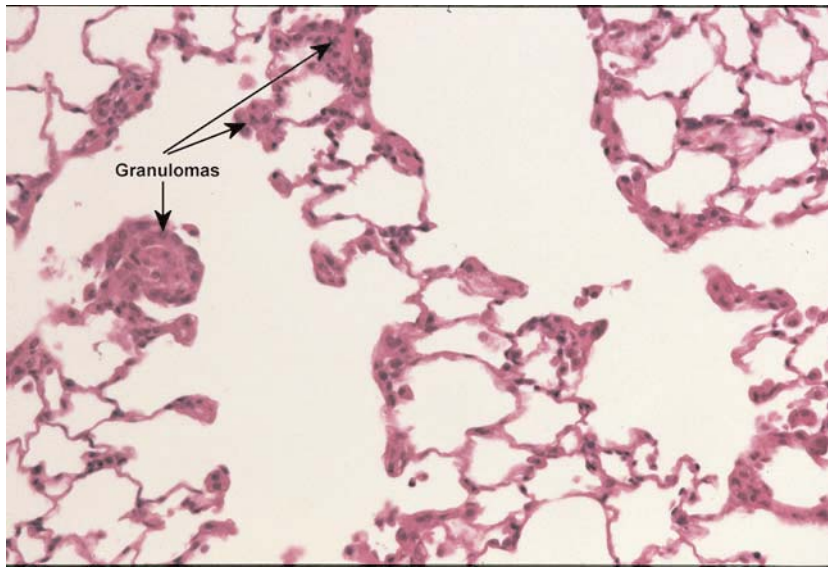


**FIGURE 13.** Photomicrograph of a histopathological section from a tremolite-exposed lung 1 day following cessation of the 5-day exposure showing the well-developed granulomatous response.

to tremolite. By day 14, the collagen deposition as seen in Figure 14 is already very apparent in the granuloma in the lung as is indicated by the arrows (The collagen is stained blue in the photomicrographs.) By 90 days after cessation of exposure, the severity of the collagen in the granulomas has increased as shown in Figures 15 and 16, in which the granuloma can be seen interlaced with collagen. By this time the collagen has progressed into the interstitium and interstitial fibrosis is seen as illustrated in Figure 15 and 16. Numerous macrophage aggregates are also observed as well as multinucleated giant cell.

In comparison, Figures 17 and 18 show the response of the lung to the Calidria chrysotile exposure at 2 and 14 days after cessation of exposure, respectively. In contrast to the tremolite-exposed lungs, no granulomas or collagen formation was seen in the Calidria chrysotile-exposed lungs. A few macrophages are seen, which is not surprising considering the recent 5 days of exposure to an atmosphere of more than 48,000 fibers/cm$^3$. Overall, the lungs of the chrysotile exposed animals were remarkable similar to the lungs of animals from the air control group that received filtered air, an example of which is shown in Figure 19.

## DISCUSSION

The Calidria mine has been a tremolite-free source of the serpentine chrysotile asbestos. The chrysotile asbestos produced from this mine has been shown to be rapidly removed following contact with the fluid lining layer of the lung.

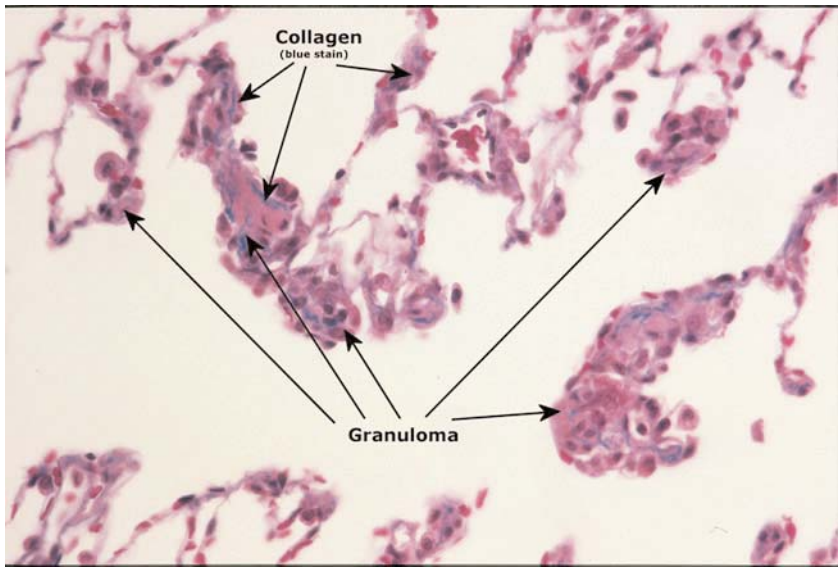


**FIGURE 14.** Photomicrograph of a histopathological section from a tremolite-exposed lung 14 days following cessation of the 5-day exposure showing the collagen deposition in the granuloma in the lung as is indicated by the arrows. (The collagen is stained blue in the photomicrographs.)

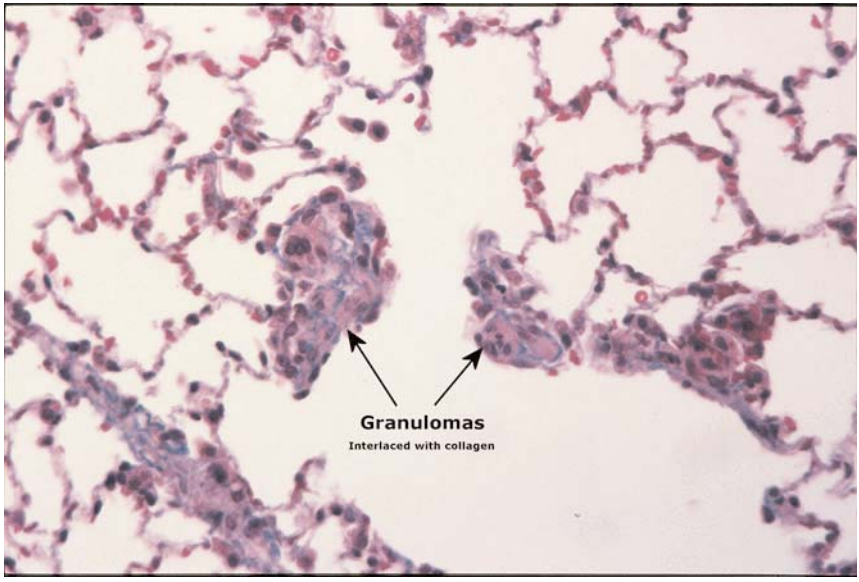


**FIGURE 15.** Photomicrograph of a histopathological section from a tremolite-exposed lung 90 days following cessation of the 5-day exposure. The severity of the collagen in the granulomas has increased and the granuloma can be seen interlaced with collagen. Numerous macrophage aggregates are also observed as well as multinucleated giant cell.

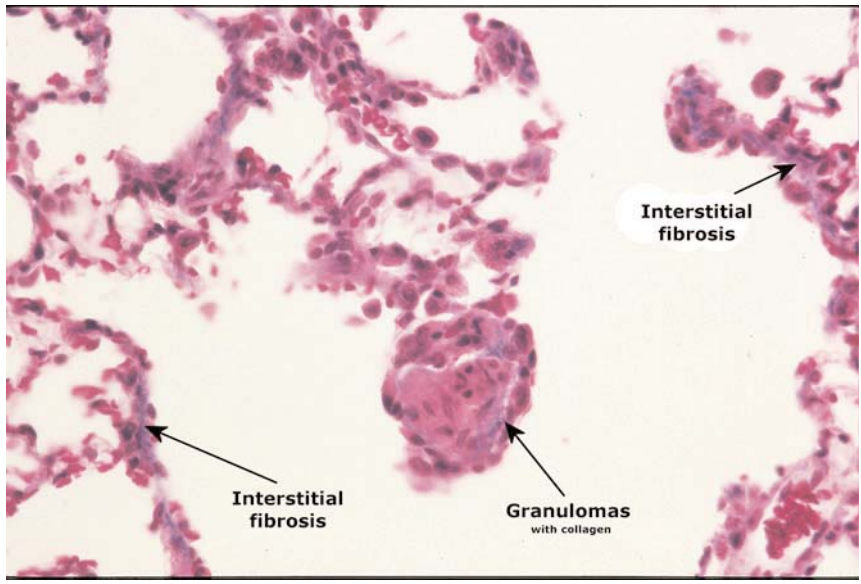


**FIGURE 16.** Photomicrograph of a histopathological section from a tremolite-exposed lung 90 days following cessation of the 5-day exposure. The severity of the collagen in the granulomas has increased and the granuloma can be seen interlaced with collagen. By this time the collagen has progressed into the interstitium and interstitial fibrosis is seen as well. Numerous macrophage aggregates are also observed as well as multinucleated giant cell.

Smith (1973) has reported that the magnesium hydroxide in the chrysotile is closest to the fiber surface while the silica tetrahedral is within the structure. He has also reported that the dissolution of chrysotile is affected by the buffer capacity of the leach solution and that the amount of extractable Mg and $SiO_2$ from chrysotile increases with increasing buffer strength. Chrysotile dissolution has been determined in vitro to be diffusion controlled through a layer of water near the mineral's surface (Swenters et al., 1985). The large buffer capacity of the lung (Matson, 1994) and the greater solubility of chrysotile in the acid environment of the macrophage would be expected to enhance dissolution further than that which has been reported in these in vitro studies (Nagy & Bates, 1952; Hume & Rimstidt, 1992).

The impervious $SiO_2$ shell-like structure of tremolite does not fall apart or dissolve upon contact with the lung's fluid lining layer and remains a rod-shaped fiber after inhalation.

That chrysotile can clear rapidly has been previously reported (Bernstein et al., 2000, 2003); however, the results of this study suggest that the Calidria chrysotile appears to disintegrate into small fibers/particles very quickly upon contact with the lung surface. The standard EC Inhalation Biopersistence protocol guidelines recommend that the first postexposure time point be 1 day after cessation of exposure. In this study, the day 0 time point immediately after cessation of exposure was added in order to provide more definition of

early clearance kinetics. Fortunately, the 0 day time point was included and this enabled the clearance half-time of the fibers longer than 20 μm to be determined as 7 h (0.3 days). By 1 day postexposure, only 1 fiber L > 20 μm was observed on the counting filter in only 1 of the 5 animals analyzed. To our knowledge, this clearance rate for Calidria chrysotile is faster than for any other fiber type reported (whether synthetic or natural). It is interesting to note that the EC Fiber Directive for which the EC Inhalation Biopersistence protocol guidelines were developed states that synthetic vitreous fibers that have a clearance half-time for fibers with length greater than 20 μm of less than 10 days are exonerated from classification as carcinogens (European Commission, 1997).

The chrysotile fibers with length ranges between 5 and 20 μm also clear rapidly with a half-time of 7 days. It would be reasonable to expect that as the longer fibers disintegrate, they contribute shorter pieces into this and shorter length fractions. The clearance half-time of 7 days for the fibers 5–20 μm in length is considerably faster than that reported by Hesterberg et al. (1998) for even soluble synthetic mineral fibers.

The objects less than 5 μm in length remaining in the lungs clear with a half-time of 59 days. This, as described earlier, is within the lower end of the range of clearance reported for insoluble inert particles following inhalation. Suquet (1989) has reported that removal through acid leaching of the magne-

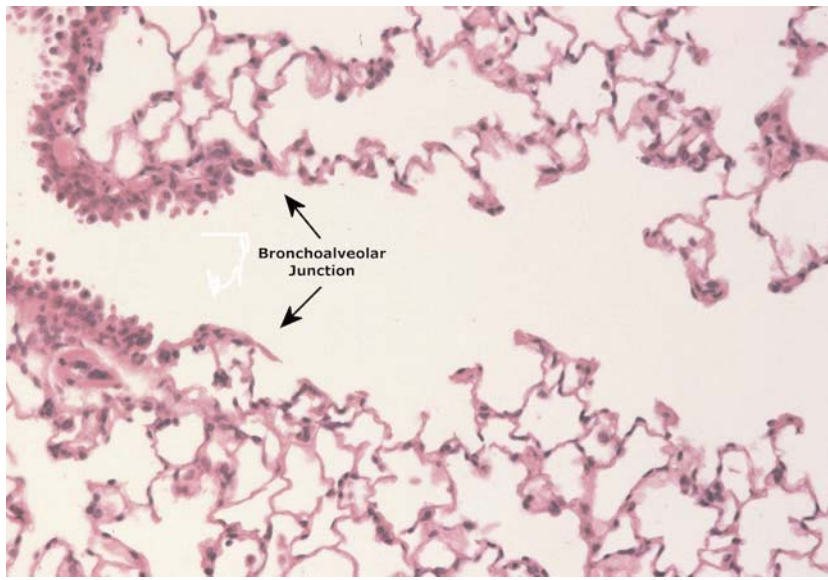


**FIGURE 17.** Photomicrograph of a histopathological section from a Calidria chrysotile exposed lung 2 days following cessation of the 5-day exposure. A few macrophages are seen which is not surprising considering the recent 5 days of exposure to an atmosphere of more than 48,000 fibers/cm$^3$. Overall, the lungs of the chrysotile exposed animals were remarkably similar to the lungs of animals from the air control group that received filtered air, an example of which is shown in Figure 19.

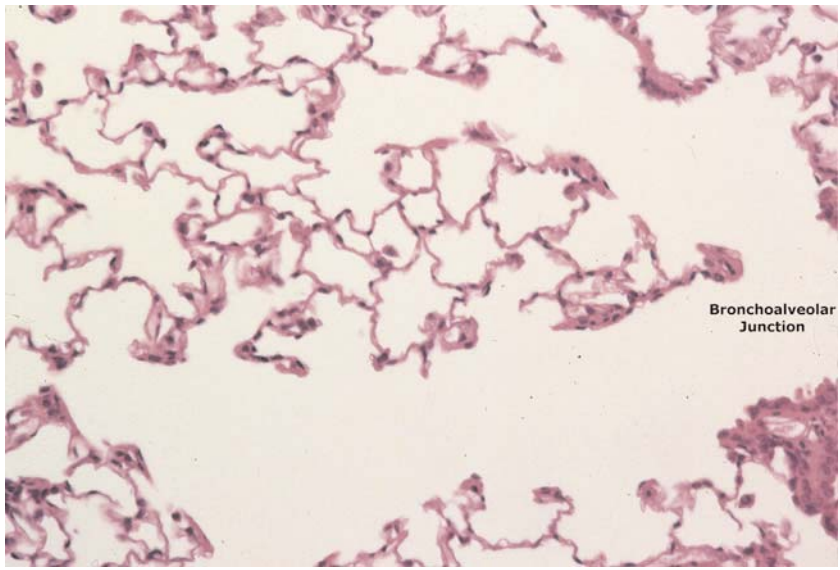


**FIGURE 18.** Photomicrograph of a histopathological section from a Calidria chrysotile exposed lung 14 days following cessation of the 5-day exposure. A few macrophages are seen which is not surprising considering the recent 5 days of exposure to an atmosphere of more than 48,000 fibers/cm$^3$. Overall, the lungs of the chrysotile exposed animals were remarkably similar to the lungs of animals from the air control group that received filtered air, an example of which is shown in Figure 19.

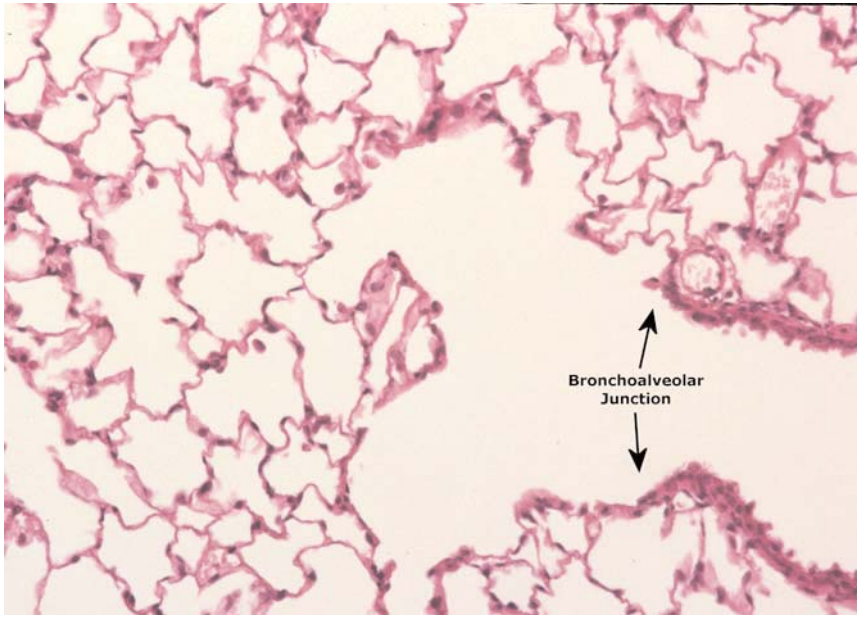


**FIGURE 19.** Photomicrograph of a histopathological section from a filtered air control lung 1 day following cessation of the 5-day filtered air exposure.

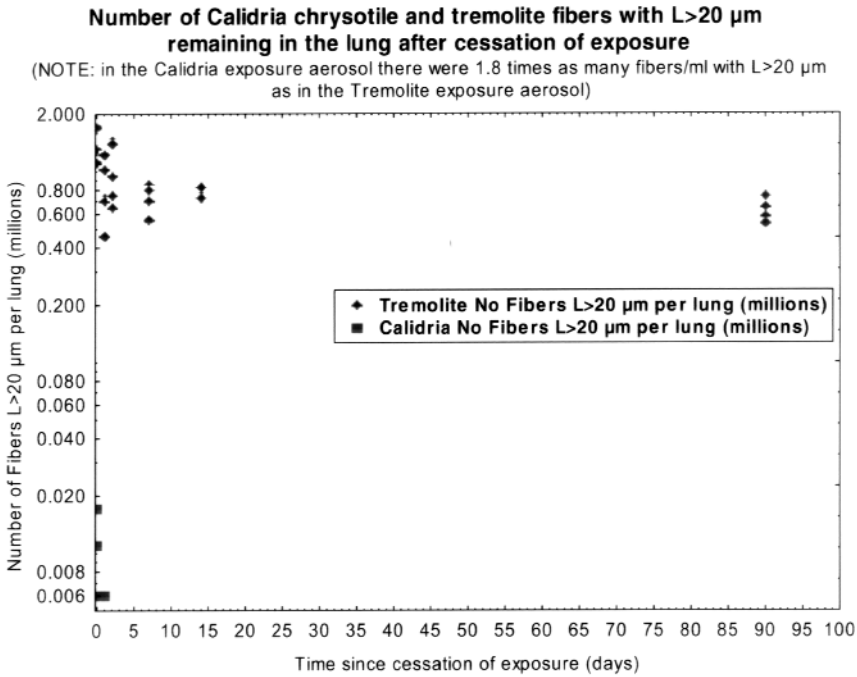


**FIGURE 20.** Graph showing the number (in millions) of Calidria chrysotile and tremolite fibers longer than 20 µm remaining in the lung following cessation of the 5-day exposure period. The Calidria chrysotile dissolves/disintegrates so fast that immediately after cessation of exposure (day 0), there is already 100 times less long chrysotile present in the lung compared to tremolite even though the chrysotile exposure atmosphere had nearly twice the concentration of fibers L > 20 µm as the tremolite exposure atmosphere.

sium oxide layers from the chrysotile fibers results in the transformation of the fiber into short fibers or particles. These shorter fibers and particles are often translocated to the lymphatics where the dissolution conditions are likely different; however, the lung digestion methodology can not distinguish between such different compartments. In addition, a recent Report on the Expert Panel on Health Effects of Asbestos and Synthetic Vitreous Fibers: The Influence of Fiber Length, issued by the Agency for Toxic Substances and Disease Registry stated that "Given findings from epidemiologic studies, laboratory animal studies, and in vitro genotoxicity studies, combined with the lung's ability to clear short fibers, the panelists agreed that there is a strong weight of evidence that asbestos and SVFs (synthetic vitreous fibers) shorter than 5 µm are unlikely to cause cancer in humans" (ATSDR, 2003; EPA, 2003).

The rapid clearance of Calidria chrysotile is reflected in the absence of any pathological response to this fiber with the lungs of the Calidria chrysotile exposed rats appearing similar to the air control rats.

With tremolite fibers longer than 20 µm, on day 1 (which is recommended by the EC protocol as the starting point for calculating clearance kinetics in

order to allow for removal of fibers which deposit on the tracheal-bronchial tree), a mean of $0.8 \times 10^6$ tremolite fibers L > 20 μm is found in the lung. With completion of this phase, there is no further clearance with approximately $0.6 \times 10^6$ fibers L > 20 μm remaining in the lung through 90 days. This difference is best illustrated as shown in Figure 20, by examination of the number of fibers with L > 20 μm remaining in the lung for tremolite and in comparison chrysotile. The Calidria chrysotile dissolves/disintegrates so fast that immediately after cessation of exposure (day 0), there is already 100 times less long chrysotile present in the lung compared to tremolite even though the chrysotile exposure atmosphere had nearly twice the concentration of fibers L > 20 μm as the tremolite exposure atmosphere. The Calidria chrysotile is clearing with a half-time of 7 h while the tremolite after the first few days does not clear further.

At 1 day after cessation of the 5-day exposure period, the rats exposed to tremolite had statistically significant elevated mean lung weights as compared to either the air control or the Calidria chrysotile-exposed rats. This is most likely a result of a large inflammatory reaction to the tremolite fibers in the lungs even during the initial days of exposure. The inflammatory reaction is reflected in the histopathology examination at day 1 after cessation of exposure with cellular lesions that were characterized by alveolar macrophage aggregation and microgranulomas. By 14 days after cessation of exposure these microgranulomas showed collagen deposition. By the next time point analyzed at 90 days postexposure the severity of the collagen deposits had increased and interstitial fibrosis was observed in one of the rats.

Both fibrotic and tumorigenic reaction to amphiboles such as crocidolite (McConnell et al., 1994) have been reported following 90 days of exposure; however, that such a short exposure to tremolite produces such a reaction is a strong indication of the reactivity of tremolite.

### Comparison with Other Studies

The differences seen in persistence and pathology in this study are also reflected in the results reported on Calidria chrysotile and on tremolite in chronic toxicology studies.

Ilgren and Chatfield (1997, 1998a, 1998b) reported on inhalation toxicology studies performed jointly by the National Institute of Environmental Health Sciences (NIEHS) of the United States Department of Health and Human Services and the Medical Research Council (MRC) Pneumoconiosis Unit in the United Kingdom to compare the results of similar inhalation studies carried out at two different locations under nearly identical conditions. As part of these studies, rats were exposed 7 h/day, 5 days/wk for 12 mo to a mean (± SD) exposure concentration of 7.8 ± 1.46 mg/m$^3$ of Coalinga chrysotile. The Coalinga chrysotile was reported as being relatively short with the majority of fibers less than 5 μm in length as found in the current study. No fibrotic or tumorigenic response was observed following exposure to the Calidria chrysotile fiber.

The results reported by Ilgren and Chatfield indicate that the total lung burden (based upon silica measurement, which is a measure of all size fibers and particles including those less than 5 μm in length) for Calidria chrysotile initially increases during the 1-yr exposure period, reaches a steady state, and then following cessation of exposure decreases steadily with approximately 95% of all size Calidria particles and fibers being cleared within 1 yr postexposure. Due to the methodology, no differentiation by fiber length was made in this study.

Similar results were reported in another chronic inhalation toxicology study of Calidria chrysotile by Muhle et al. (1987) in which rats were exposed to a concentration of 6 mg/m$^3$ of Calidria chrysotile for 5 h, 4 times/wk for 1 yr with subgroups of rats retained through an additional 1 yr postexposure. The authors reported that no significant increase in tumors occurred from exposure to the Calidria chrysotile. The Calidria chrysotile fiber was also tested in four chronic intraperitoneal injection (ip) studies at doses of up to 3 mg with tumor levels in the reported background range of up to 10% (Muhle et al., 1987; Pott et al., 1987; Rittinghausen et al., 1992). These studies provide support that Calidria chrysotile is not carcinogenic following both inhalation and ip exposure at relatively high concentrations.

The response to the chronic inhalation exposure of tremolite fiber similar to that used in the current study was reported by Davis et al. (1985). Rats were exposed for 7 h/day, 5 days/wk for 12 mo to Korean tremolite aerosol concentration of 10 mg/m$^3$, which was documented as having 1600 fibers L > 5 μm/cm$^3$ as measured by phase-contrast optical microscopy (PCOM). Groups of rats were examined histopathologically at 12, 18, and 27–29 mo. From Figure 1 in the Davis et al. publication, there were approximately 270 fibers L > 20 μm/cm$^3$ in the exposure atmosphere as measured by PCOM. When using scanning electron microscopy, there were approximately 3% of the fibers with length greater than 20 μm, which corresponds very closely with the results of the current study of 3.4% by TEM. The rats treated with tremolite developed very high levels of pulmonary fibrosis as well as 16 carcinomas and 2 mesotheliomas in a group of 39 animals. The authors reported that "tremolite thus proved to be the most dangerous mineral that we have studied."

## CONCLUSIONS

These findings provide an important basis for substantiating both kinetically and pathologically the differences between chrysotile and the amphibole tremolite.

Following this 5-day exposure to tremolite the tremolite fibers once deposited in the lung parenchyma do not clear and almost immediately result in inflammation and a pathological response in the lung. At the first time point examined, 1 day after cessation of exposure, cellular change and granulomas were already formed. By 14 days postexposure these lesions had turned fibrotic, and by 90 days postexposure had developed into interstitial fibrosis. As

the tremolite fibers do not clear from the lung and remain as a persistent source for pathological stimulation, it will be most interesting to follow the subsequent evolution of the pathological lesions at 6 and 12 mo postexposure.

While chrysotile has been shown previously to clear rapidly (Bernstein et al., 2000, 2003), the Calidria chrysotile fibers clear from the lung more rapidly ($T_{1/2,\ \text{fibers L>20 μm}} = 7$ h) than any other commercial fiber tested including synthetic mineral fibers. With such rapidly clearing fibers, the 5-day exposure would not be expected to result in any pathological change in the lung and as reported earlier, the lungs of animals that inhaled Calidria chrysotile showed no sign of inflammation or pathology and were no different than the lungs of those animals that breathed filtered air.

This study provides a strong mechanistic basis for the epidemiological differences reported between chrysotile and amphiboles. McDonald et al. (2003; McDonald & McDonald, 1997) reported that the occupational risks of both mesothelioma and lung cancer are related to estimated levels of tremolite in the mines where the men had worked and the current study provides additional support for this differentiation. As Calidria chrysotile has been certified to have no tremolite fiber, the results of the current study together with the results from toxicological and epidemiological studies indicate that this fiber is not associated with lung disease.

## APPENDIX

**TABLE A1.** Summary incidence of histopathological findings (1 day after cessation of exposure)

| | Air control | Calidria chrysotile | Tremolite |
|---|---|---|---|
| Number animals per dose group examined | 3 | 5 | 5 |
| Lung | | | |
| Alveolar histiocytosis: reactive; focal/multifocal | | | |
| Grade 2 | — | — | 3 |
| Grade 3 | — | — | 2 |
| Total affected | — | — | 5 |
| Mean severity | — | — | 2.4 |
| Granuloma: bronchiolo-alveolar junction | | | |
| Grade 2 | — | — | 2 |
| Grade 3 | — | — | 3 |
| Total affected | — | — | 5 |
| Mean severity | — | — | 2.6 |
| Alveolar lining cell hypertrophy/hyperplasia | | | |
| Grade 2 | — | — | 1 |
| Grade 3 | — | — | 1 |
| Total affected | — | — | 2 |
| Mean severity | — | — | 2.5 |
| Bronchiolitis | | | |
| Grade 1 | — | — | 1 |
| Grade 2 | — | — | 3 |
| Total affected | — | — | 4 |
| Mean severity | — | — | 1.8 |

**TABLE A2.** Summary incidence of histopathological findings (2 days after cessation of exposure)

| | Air control | Calidria chrysotile | Tremolite |
|---|---|---|---|
| Number animals per dose group examined | 3 | 5 | 5 |
| Lung | | | |
| Alveolar histiocytosis: reactive; focal/multifocal | | | |
| Grade 3 | — | — | 5 |
| Total affected | — | — | 5 |
| Mean severity | — | — | 3.0 |
| Granuloma: bronchiolo-alveolar junction | | | |
| Grade 3 | — | — | 5 |
| Total affected | — | — | 5 |
| Mean severity | — | — | 3.0 |
| Alveolar lining cell hypertrophy/hyperplasia | | | |
| Grade 2 | — | — | 5 |
| Total affected | — | — | 5 |
| Mean severity | — | — | 2.0 |
| Bronchiolitis | | | |
| Grade 2 | — | — | 4 |
| Grade 3 | — | — | 1 |
| Total affected | — | — | 5 |
| Mean severity | — | — | 2.2 |
| Alveolar hemorrhage | | | |
| Grade 2 | — | 1 | — |
| Total affected | — | 1 | — |
| Mean severity | — | 2.0 | — |

**TABLE A3.** Summary incidence of histopathological findings (14 days after cessation of exposure)

| | Air control | Calidria chrysotile | Tremolite |
|---|---|---|---|
| Number animals per dose group examined | 3 | 5 | 5 |
| Lung | | | |
| Alveolar histiocytosis: reactive; focal/multifocal | | | |
| Grade 2 | — | — | 2 |
| Grade 3 | — | — | 3 |
| Total affected | — | — | 5 |
| Mean severity | — | — | 2.6 |
| Foam-cell aggregation: focal/multifocal | | | |
| Grade 2 | — | 1 | — |
| Grade 3 | — | 1 | — |
| Total affected | — | 2 | — |
| Mean severity | — | 2.5 | — |
| Granuloma: bronchiolo-alveolar junction | | | |
| Grade 3 | — | — | 5 |
| Total affected | — | — | 5 |
| Mean severity | — | — | 3.0 |
| Multinucleated giant cells in granulomas | | | |
| Grade 2 | — | — | 2 |
| Total affected | — | — | 2 |
| Mean severity | — | — | 2.0 |

(*Table continues on next page*)

**TABLE A3.** Summary incidence of histopathological findings (14 days after cessation of exposure) (*continued*)

| | Air control | Calidria chrysotile | Tremolite |
|---|---|---|---|
| Lungs, trichrome | | | |
| Collagen in granulomas | | | |
| Grade 1 | — | — | 3 |
| Grade 2 | — | — | 1 |
| Total affected | — | — | 4 |
| Mean severity | — | — | 1.3 |

**TABLE A4.** Summary incidence of histopathological findings (90 days after cessation of exposure)

| | Air control | Calidria chrysotile | Tremolite |
|---|---|---|---|
| Number animals per dose group examined | 3 | 4 | 4 |
| Lung | | | |
| Alveolar histiocytosis: reactive; focal/multifocal | | | |
| Grade 2 | — | — | 1 |
| Total affected | — | — | 1 |
| Mean severity | — | — | 2.0 |
| Foam-cell aggregation: focal/multifocal | | | |
| Grade 2 | — | 2 | — |
| Total affected | — | 2 | — |
| Mean severity | — | 2.0 | — |
| Granuloma: bronchiolo-alveolar junction | | | |
| Grade 2 | — | — | 1 |
| Grade 3 | — | — | 3 |
| Total affected | — | — | 4 |
| Mean severity | — | — | 2.8 |
| Lungs, trichrome | | | |
| Collagen in granulomas | | | |
| Grade 2 | — | — | 1 |
| Grade 3 | — | — | 3 |
| Total affected | — | — | 4 |
| Mean severity | — | — | 2.8 |
| Interstitial collagen deposition | | | |
| Grade 2 | — | — | 1 |
| Total affected | — | — | 1 |
| Mean severity | — | — | 2.0 |
| Mediast. lymph node | | | |
| Histiocytosis | | | |
| Grade 3 | — | — | 1 |
| Total affected | — | — | 1 |
| Mean severity | — | — | 3.0 |
| Erythro-phagocytosis | | | |
| Grade 2 | — | — | 1 |
| Total affected | — | — | 1 |
| Mean severity | — | — | 2.0 |

## REFERENCES


ATSDR. 2003. *Report on the Expert Panel on Health Effects of Asbestos and Synthetic Vitreous Fibers: The influence of fiber length.* Prepared for Agency for Toxic Substances and Disease Registry Division of Health Assessment and Consultation Atlanta, GA.

Bernstein, D. M., Rogers, R., and Smith, P. 2003. The biopersistence of Canadian chrysotile asbestos following inhalation. *Inhal. Toxicol.* 15(13):1247-1274.

Bernstein, D. M., and Riego-Sintes, J. M. R. 1999. *Methods for the determination of the hazardous properties for human health of man made mineral fibers (MMMF).* European Commission Joint Research Centre, Institute for Health and Consumer Protection, Unit: Toxicology and Chemical Substances, European Chemicals Bureau, EUR 18748 EN, April. http://ecb.ei.jrc.it/DOCUMENTS/Testing-Methods/mmmfweb.pdf

Bernstein, D. M., Mast, R., Anderson, R., Hesterberg, T. W., Musselman, R., Kamstrup, O., and Hadley, J. 1994. An experimental approach to the evaluation of the biopersistence of respirable synthetic fibers and minerals. *Environ. Health Perspect.* 102(suppl. 5):15–18.

Bernstein, D. M., Rogers, R., and Thevenaz, P. 2000. The inhalation biopersistence and morphologic lung disposition of pure chrysotile asbestos in rats. *Toxicol. Sci. Toxicologist* 54(1):318.

Bernstein, D. M., Riego-Sintes, J. M., Ersboell, B. K., and Kunert, J. 2001a. Biopersistence of synthetic mineral fibers as a predictor of chronic inhalation toxicity in rats. *Inhal. Toxicol.* 13(10):823–849.

Bernstein, D. M., Riego-Sintes, J. M., Ersboell, B. K., and Kunert, J. 2001b. Biopersistence of synthetic mineral fibers as a predictor of chronic intraperitoneal injection tumor response in rats. *Inhal. Toxicol.* 13(10):851–875.

Campbell, W. J., Huggins, C. W., and Wylie, A. G. 1980. *Chemical and physical characterization of amosite, chrysotile, crocidolite, and nonfibrous tremolite for oral ingestion studies by the National Institute of Environmental Health Sciences.* Nevada Bureau of Mines Report of Investigation, No. 8452. Washington, DC: Nevada Bureau of Mines.

Cannon, W. C., Blanton, E. F., and McDonald, K. E. 1983. The flow-past chamber: An improved nose-only exposure system for rodents. *Am. Ind. Hyg. Assoc. J.* 44(12):923–928.

Churg, A. 1994. Deposition and clearance of chrysotile asbestos. *Ann. Occup. Hyg.* 38(4):625–633.

Churg, A., and DePaoli, L. 1988. Clearance of chrysotile asbestos from human lung. *Exp. Lung Res.* 14:567–574.

Coleman, R. G. 1996. New Idria serpentinite: A land management dilemma. *Environ. Eng. Geosci.* II(1):9–22.

Davis, J. M. G., Addison, J., Bolton, R. E., Donaldson, K., Jones, A. D., and Miller, B. G. 1985. Inhalation studies on the effects of tremolite and brucite dust in rats. *Carcinogenesis* 6(5): 667–674.

European Commission. 1997. O.J. L 343/19 of 13 December 1997. Commission Directive 97/69/EC of 5 December 1997 adapting to technical progress for the 23rd time Council Directive 67/548/EEC on the approximation of the laws regulations and administrative provisions relating to the classification, packaging and labelling of dangerous substances.

Hesterberg, T. W., Chase, G., Axten, C., Miiller, W. C., Musselman, R. P., Kamstrup, O., Hadley, J., Morscheidt, C., Bernstein, D. M., and Thevenaz, P. 1998. Biopersistence of synthetic vitreous fibers and amosite asbestos in the rat lung following inhalation. *Toxicol. Appl. Pharmacol.* 151(2): 262–275.

Hodgson, A. A. 1979. Chemistry and physics of asbestos. In *Asbestos: Properties, applications and hazards,* eds. L. Michaels and S. S. Chissick, pp. 80–81. New York: John Wiley & Sons.

Hodgson, J. T., and Darnton, A. 2000. The quantitative risks of mesothelioma and lung cancer in relation to asbestos exposure. *Ann. Occup. Hyg.* 44(8):565–601.

Howard, J. K. 1984. Relative cancer risks from exposure to different asbestos fibre types. *N. Z. Med. J.* 97:646–649.

Hume, L. A., and Rimstidt, J. D. 1992. The biodurability of chrysotile asbestos. *Am. Miner.* 77:1125–1128.

Ilgren, E. 2002. Coalinga fibre—A short, amphibole-free chrysotile, Part 4: Further evidence for a lack of fibrogenic and tumorigenic activity. *Indoor Built Environ.* 11:171–177.

Ilgren, E., and Chatfield, E. 1997. Coalinga fibre—A short, amphibole-free chrysotile, Part 1: Evidence for a lack of fibrogenic activity. *Indoor Built Environ.* 6:264–276.

Ilgren, E., and Chatfield, E. 1998a. Coalinga fibre: A short, amphibole-free chrysotile, Part 3: Lack of biopersistence. *Indoor Built Environ.* 7:98–109.

Ilgren, E., and Chatfield, E. 1998b. Coalinga fibre—A short, amphibole-free chrysotile, Part 2: Evidence for lack of tumourigenic activity. *Indoor Built Environ.* 7:18–31.

Matson, S. M. 1994. Glass fibres in simulated lung fluid: Dissolution behavior and analytical requirements. *Ann. Occup. Hyg.* 38:857–877.

McConnell, E. E., Kamstrup, O., Musselman, R., Hesterberg, T. W., Chevalier, J., Miiller, W. C., and Thevanaz, P. 1994. Chronic inhalation study of size-separated rock and slag wool insulation fibers in Fischer 344/N rats. *Inhal. Toxicol.* 6(6):571–614.

McDonald, J. C. 1998. Mineral fibre persistence and carcinogenicity. *Ind. Health* 36(4):372–375.

McDonald, J. C., and McDonald, A. D. 1997. Chrysotile, tremolite and carcinogenicity. *Ann. Occup. Hyg.* 41(6):699–705.

McDonald, J. C., McDonald, A. D., and Hughes, J. M. 1999. Chrysotile, tremolite and fibrogenicity. *Ann. Occup. Hyg.* 43(7):439–442.

McDonald, J. C, Harris, J., and Armstrong, B. 2002. Cohort mortality study of vermiculite miners exposed to fibrous tremolite: An update. *Ann. Occup. Hyg.* 46(suppl. 1):93–94.

McDonald, J. C., Harris, J., and Armstrong, B., 2003. Mortality in a cohort of Montana vermiculite miners exposed to fibrous tremolite. *Occup. Environ. Med.,* in press.

Morgan, A. 1994. The removal of fibres of chrysotile asbestos from lung. *Ann. Occup. Hyg.* 38(4):643–646.

Mossman, B. T., Bignon, J., Corn, M., Seaton, A., and Gee, J. B. L. 1990. Asbestos: Scientific developments and implications for public policy. *Science* 247:294–301.

Muhle, H., Pott, F., Bellmann, B., Takenaka, S., and Ziem, U. 1987. Inhalation and injection experiments in rats to test the carcinogenicity of MMMF. *Ann. Occup. Hyg.* 31(4B):755–764.

Muhle, H., Creutzenberg, O., Bellmann, B., Heinrich, U., and Mermelstein, R. 1990. Dust overloading of lungs: Investigations of various materials, species differences, and irreversibility of effects. *J. Aerosol Med.* 3(suppl. 1):111–128.

Mumpton, F. A., and Thompson, C. S. 1975. Mineralogy and origin of the Coalinga asbestos deposit. *Clays Clay Miner.* 23:131–143.

Nagy, B., and Bates, T. F. 1952. Stability of chrysotile asbestos. *Am. Mineral.* 37:1055–1058.

Oberdoerster, G. 1994. Macrophage associated responses to chrysotile. *Ann. Occup. Hyg.* 38(4):601–615.

Pooley, F. 2003. Personal communication of a report prepared under contract to KCAC of the examination of chrysotile asbestos samples from the asbestos mine and processing plant of KCAC, Inc., 1991.

Pott, F., Ziem, U., Reiffer, F. J., Huth, F., Ernst, H., and Mohr, U. 1987. Carcinogenicity studies on fibres, metal compounds, and some other dusts in rats. *Exp. Pathol.* 32(3):129–152.

Rittinghausen, S., Ernst, H., Muhle, H., and Mohr, U. 1992. Atypical malignant mesotheliomas with osseous and cartilaginous differentiation after intraperitoneal injection of various types of mineral fibres in rats. *Exp. Toxicol. Pathol.* 44(1):55–58.

Rodelsperger, K., Woitowitz, H. J., Bruckel, B., Arhelger, R., Pohlabeln, H., and Jockel, K. H. 1999. Dose-response relationship between amphibole fiber lung burden and mesothelioma. *Cancer Detect. Prev.* 23(3):183–193.

Rogers, R. A., Antonini, J. M., Brismar, H., Lai, J., Hesterberg, T. W., Oldmixon, E. H., Thevenaz, P., and Brain, J. D. 1999. In situ microscopic analysis of asbestos and synthetic vitreous fibers retained in hamster lungs following inhalation. *Environ. Health Perspect.* 107(5):367–375.

Skinner, H. C. W., Ross, M., and Frondel, C., eds. 1988. *Asbestos and other fibrous minerals.* Oxford University Press, pp. 30–32 and Figure 2–3.

Smith, R. W. April 1973. *Aqueous surface chemistry of asbestos minerals, final progress report.* University of Nevada, Reno. NTIS number PB90100942. April.

Stöber, W., Morrow, P. E., Morawietz, G., Koch, W., and Hoover, M. D. 1990. Developments in modeling alveolar retention of insoluble particles in rats. *J. Aerosol. Med.* 3(suppl. 1):S129–S154.

Suquet, H. 1989. Effects of dry grinding and leaching on the crystal structure of chrysotile. *Clays Clay Miner.* 31(5):439–445.

Swenters, I. M., De Waele, J. K., Verlinden, J. A. and Adams, F. C. 1985. Comparison of secondary-ion mass spectrometry and romplexiметric titration for the determination of leaching of magnesium from chrysotile asbestos. *Anal. Chim. Acta* 173:377–380.

U.S. Environmental Protection Agency. 2003. *Report on the Peer Consultation Workshop to discuss a proposed protocol to assess asbestos-related risk.* Prepared for U.S. Environmental Protection Agency, Office of Solid Waste and Emergency Response, Washington, DC 20460, EPA Contract No. 68-C-98-148, Work Assignment 2003-05. Prepared by Eastern Research Group, Inc., 110 Hartwell Avenue, Lexington, MA 02421. Final Report May 30, 2003.

Wicks, F. J., and O'Hanley, D. S. 1988. Serpentine minerals: Structures and petrology. Reviews in mineralogy. Hydrous phyllosilicates. *Am. Mineral.* 19:91–167.

World Health Organization. 1985. *World Health Organization, Reference Methods for Measuring Airborne Man-Made Mineral Fibres (MMMF).* WHO/EURO MMMF Reference Scheme prepared by the WHO/EURO Technical Committee for Monitoring and Evaluating Airborne MMMF, Copenhagen.

Yu, C. P., Zhang, L., Oberdorster, G., Mast, R. W., Glass, L. R., and Utell, M. J. 1994. On the clearance of refractory ceramic fibers (RCF) from the rat lung. Development of a model. *J. Environ. Res.* 65: 243–253.